Nonisothermal Crystallization Behavior of Highly Exfoliated Polypropylene/Clay Nanocomposites Prepared by *In Situ* Polymerization

Xin Liu,[1] Aihua He,[2] Kai Du,[1] Charles C. Han[1]

[1]*State Key Laboratory of Polymer Physics and Chemistry, Joint Laboratory of Polymer Science and Materials, Beijing National Laboratory for Molecular Sciences, Institute of Chemistry, Chinese Academy of Sciences, Beijing 100190, China*
[2]*Key Laboratory of Rubber-Plastics (Ministry of Education), School of Polymer Science and Engineering, Qingdao University of Science and Technology, Qingdao 266042, China*

Received 27 November 2009; accepted 21 February 2010
DOI 10.1002/app.32335
Published online 21 July 2010 in Wiley Online Library (wileyonlinelibrary.com).

ABSTRACT: Polypropylene/clay nanocomposites (PPCNs) were prepared via an *in situ* polymerization method with a Ziegler–Natta/clay compound catalyst in which the $MgCl_2/TiCl_4$ catalyst was embedded in the clay galleries. The wide-angle X-ray diffraction and transmission electron microscopy results showed that the clay particles were highly exfoliated in the polypropylene (PP) matrix. The nonisothermal crystallization kinetics of these PPCNs were investigated by differential scanning calorimetry at various cooling rates. The nucleation activity were calculated by Dobreva's method to demonstrate that the highly dispersed silicate layers acted as effective nucleating agents. The Avrami, Jeziorny, Ozawa, and Mo methods were used to describe the nonisothermal crystallization behavior of the PP and PPCNs. Various parameters of nonisothermal crystallization, such as the crystallization half-time, crystallization rate constant, and the kinetic parameter $F(t)$, reflected that the highly exfoliated silicate layers significantly accelerated the crystallization process because of its outstanding nucleation effect. The activation energy values of the PP and PPCNs determined by the Kissinger method increased with the addition of the nanosilicate layers. © 2010 Wiley Periodicals, Inc. J Appl Polym Sci 119: 162–172, 2011

Key words: clay; crystallization; kinetics (polym.); nanocomposites; poly(propylene) (PP)

INTRODUCTION

Polymer/clay nanocomposites with clay particles typically in the range 1–200 nm exhibit various properties, such as strength, gas permeability, thermal stability, and electrical properties, that are superior to those of conventional microsized composites because of the nanosize effects.[1–6] Polypropylene (PP) is a kind of widely used engineering plastic. However, the congenital deficiencies of PP, such as its toughness and barrier properties, limit its applications in automotive and packaging materials. Therefore, the use of clay particles to enhance the properties of PP has attracted lots of attention.

The mechanical properties of polymer products greatly depend on the crystallization behavior and crystal structure, so studies of the crystallization process of polypropylene/clay nanocomposites (PPCNs) are hot issues. To date, most studies have focused on intercalated PPCNs.[7–16] Nam et al.[15] prepared intercalated PPCNs using pure PP, maleic anhydride modified polypropylene (MA–PP), and organic clay via a melt-extrusion process. They found that the PPCNs formed a rodlike crystalline texture that included γ-phase crystallites. They assumed that the formation of γ-phase crystallites was caused by the reduction of MA–PP chain mobility due to the intercalation of the PP chains in the space between silicate galleries and the narrow space around the clay particles. When a fine clay dispersion was achieved with MA–PP, the clay-nucleating effect was limited, and a lower crystallization temperature (T_c) and crystallization rates were observed.[8] Maiti et al.[14] at the Toyota center studied intercalated PPCNs and found that the intercalative clay acted as a nucleating agent in the PP matrix. A similar nucleating effect was also described elsewhere.[13] The extent of intercalation of polymer chains into silicate galleries increased with T_c for any clay content in the PPCNs, and at a constant T_c, the extent of intercalation increased with decreasing clay content.

Perrin-Sarazin et al.[8] prepared PPCNs via melt blending using different clays and compatibilizers

Correspondence to: A. He (aihuahe@iccas.ac.cn).
Contract grant sponsor: National Nature Science Foundation of China; contract grant number: 20774098.
Contract grant sponsor: National '973' Project; contract grant number: G2003 CB615605.

TABLE I
Basic Physical Parameters of the Commercial PP and PPCNs

Sample	Clay (wt %)	T_m (°C)	Isotactic index (%)
Pure PP	0	166.1	>95
PP/clay1	1.3	162.8	89.2
PP/clay2	2.2	162.6	92.7
PP/clay3	4.8	162.2	92.6

based on MA–PP. They found that clay induced some orientation of α-phase PP crystallites.

Ma et al.[16] studied the isothermal crystallization kinetics of partially exfoliated PP/montmorillonite(MMT) nanocomposites via propylene polymerization. They found that the PP chains were confined by the MMT layers, the crystallinity was reduced, and the spherulite size was decreased with increasing MMT content.

Isothermal and nonisothermal kinetic analysis is commonly used to study the crystallization behavior of polymer/clay nanocomposites. Compared with that of isothermal crystallization, the study of nonisothermal crystallization is much more complicated because one more variable, the temperature as a function of time, must be considered. The study of nonisothermal crystallization in polymer/clay nanocomposites is of greater practical significance because the final properties of polymer/clay nanocomposites are dependent on the processing conditions and the processing procedures always involve the nonisothermal crystallization process. Recently, the nonisothermal crystallization kinetics of many polymer/clay nanocomposites have been studied; these composites include poly(ethylene oxide)/MMT,[17] polyamide 66/clay,[18] *in situ* polymerized polyethylene/clay,[19] poly(trimethylene terephthalate)/clay,[20] intercalative PP/MMT,[12,13] and polyamide 6/clay.[21,22] Clay was found to have two mutually opposite effects on the polymer crystallization behavior: crystallization nucleating promotion and crystallization growth retardation.

However, the nonisothermal crystallization behavior of highly exfoliated PPCNs without any compatibilizer is still unclear. The investigation of this system could provide further understanding of the relationship between the nanosilicate layers and polymer crystallization. In our previous studies,[23–25] exfoliated PPCNs were successfully prepared via a novel *in situ* polymerization method. In this study, several nonisothermal crystallization kinetic models were used to investigate the crystallization behavior of PP and highly exfoliated PPCNs; the models we used included those of Dobreva,[26,27] Avrami,[28] Jeziorny,[29] Ozawa,[30] and Mo.[31] The activation energies (ΔE's) of the PP and PPCNs were also calculated by the Kissinger method.[32]

EXPERIMENTAL

Materials

PPCNs with clay contents of 1.3, 2.2, and 4.8 wt % were synthesized via an *in situ* polymerization method.[33] In the preparation, a Ziegler–Natta type of Ti catalyst was embedded in the clay galleries, and the exfoliated PPCNs were synthesized. The clay was produced by Qinghe Chemical Plant (Zhangjiakou Hebei province China). The cation-exchange capacity of the clay was 90 mequiv/100 g. The lateral dimensions of the clay layers were 50–200 nm.[33]

A commercial-grade pure iPP (S1003) was kindly supplied by Yanshan Petrochemical Co., Ltd. (Beijing, China).

The basic sample physical parameters are listed in Table I.

Characterization

Wide-angle X-ray diffraction (WAXD) experiments were performed with a D8 advance X-ray powder diffractometer (Bruker Co. Madison, WI USA) with Cu Kα radiation ($\lambda = 0.154$ nm) at a generator voltage of 40 kV and a generator current of 40 mA. The scanning rate was 2°/min. The interlayer spacing (d_{001}) of clay was calculated in accordance with the Bragg equation: $2d \sin\theta = \lambda$, where λ is the wavelength of incident wave, d is the spacing between the planes in the atomic lattic, and θ is the angle between the incident ray and the scattering planes.

Transmission electron microscopy (TEM) was carried out on a Jeol JEM2200FS transmission electron microscope (Tokyo, Japan) with an acceleration voltage of 200 kV. Samples for TEM were prepared by embedding in epoxy resin and microtomed into ultrathin sections.

Differential scanning calorimetry (DSC) was conducted with a Perkin-Elmer DSC-7 (Waltham, MA USA) thermal analyzer. The temperature and heat flow were calibrated with indium at each cooling rate (ϕ) used in the measurements. All measurements were carried out in a nitrogen atmosphere. For nonisothermal crystallization, all samples were heated to 200°C at a heating rate of 10°C/min and held at 200°C for 10 min to eliminate the influence of the thermal history. Then, the samples were cooled at ϕ values of 5, 10, 20, 30, and 40°C/min respectively. The exothermic crystallization peak was recorded as a function of temperature.

RESULTS AND DISCUSSION

Characterization of the PPCNs

As shown in Figure 1(a–c),[33] the lateral dimensions of the clay layers were within the range 50–200 nm; and

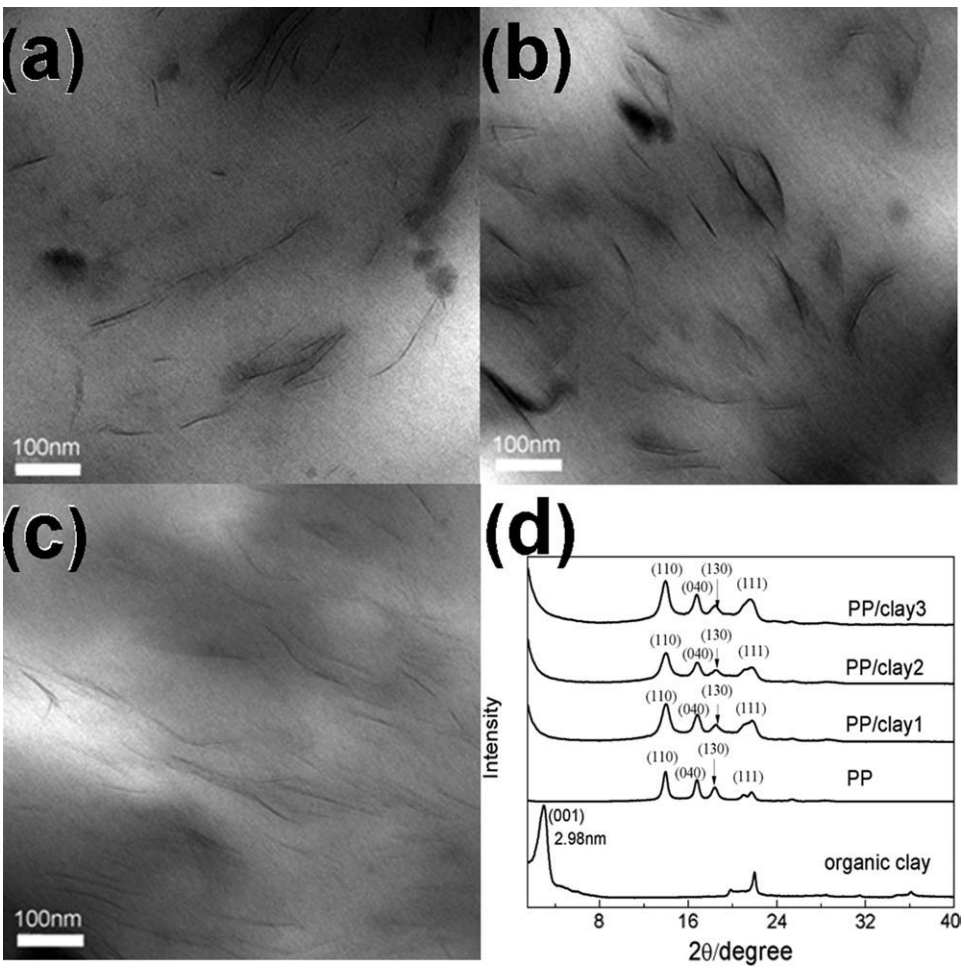

Figure 1 TEM images of the nanocomposites, (a) PP/clay1 1.3 wt %, (b) PP/clay2 2.2 wt %, and (c) PP/clay3 4.8 wt %, and (d) WAXD patterns of organic clay, pure PP, and PPCNs.

the thickness of the silicate particles were less than 10 nm. Because the thickness of a single silicate layer was around 1 nm,[34,35] which was of the same order of magnitude as what we observed, as shown in Figure 1, the clay particles were exfoliated into nanosilicate layers during the *in situ* polymerization process. The WAXD patterns [Fig. 1(d)] showed that the d_{001} values in these nanocomposites were larger than 5.9 nm. Therefore, we concluded that the originally stacked clay particles were highly exfoliated in the PP matrix.

Nonisothermal crystallization behavior of the PP and PPCNs

The nonisothermal crystallization behavior of the PP and exfoliated PPCNs were quantitatively analyzed through DSC experiments. Figure 2 shows the crystallization exotherms of the PP and PPCNs at selected ϕ values of 5, 10, 20, 30, and 40°C/min, respectively. From these curves, the T_c, crystallization peak temperature (T_P), and crystallization enthalpy (ΔH_c) were determined. The results are summarized in Table II.

At a lower ϕ values, there was a longer time for PP to overcome the nucleation energy barrier, and the motion of the PP molecules followed the cooling temperature better than at higher ϕ values. Therefore, as shown in Table II, T_c and T_P of the PP and PPCNs both decreased with increasing ϕ. It is also shown in Table II that at a given ϕ, T_c and T_P of the PPCNs shifted toward higher temperatures compared with those of PP. This was because the exfoliated clay particles acted as effective heterogeneous nucleating agents and accelerated the crystallization process of PP.[19,33]

Dobreva and Gutzow[26,27] described a simple method to calculate ε of the filler. For homogeneous nucleation during the nonisothermal crystallization process, the following relationships were proposed:

$$\log \phi = A - \frac{B}{2.3\Delta T_P^2} \quad (1)$$

In the case of heterogeneous nucleation[26,27]

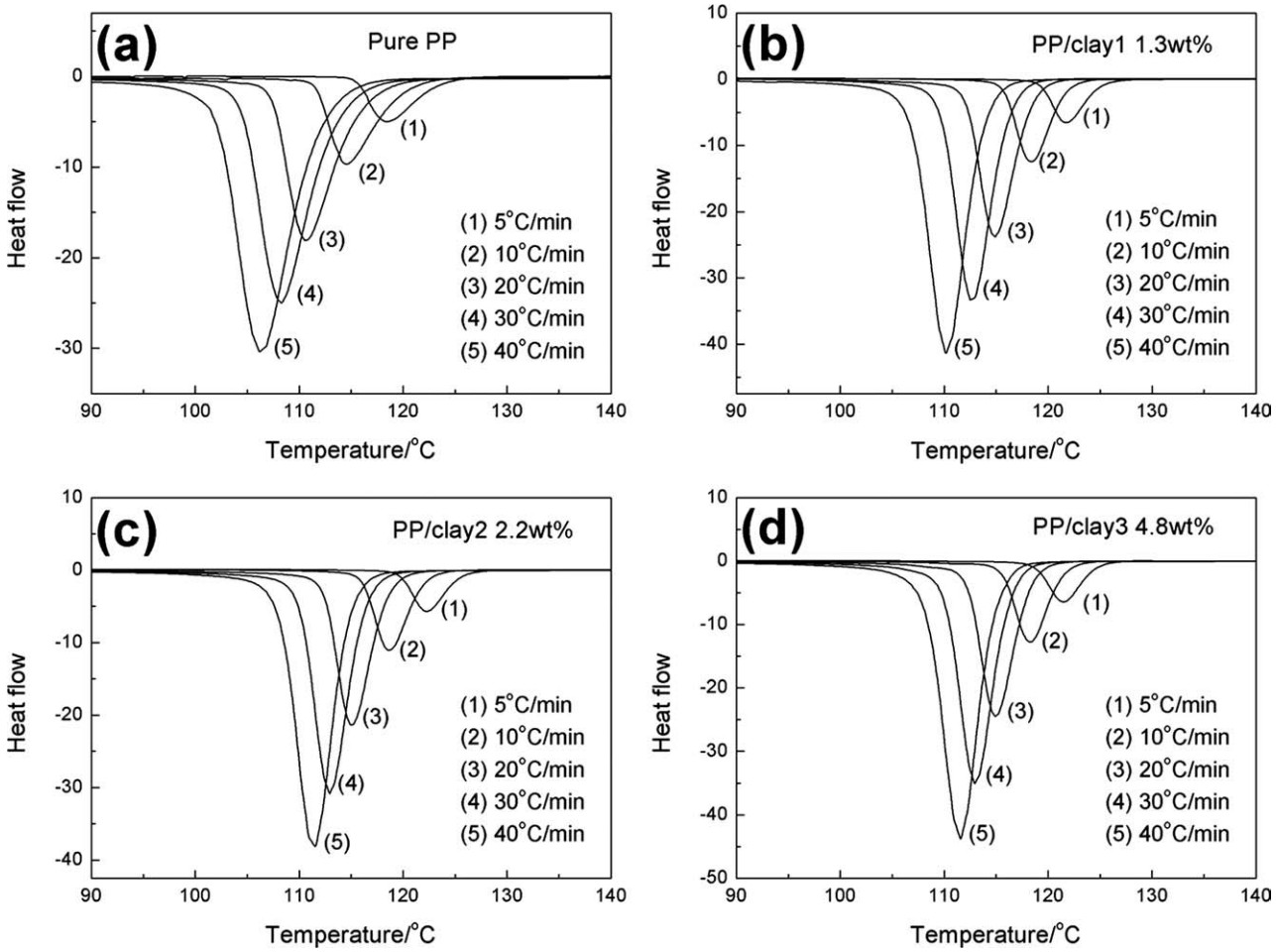

Figure 2 Nonisothermal crystallization exotherms of the PP and PPCNs at ϕ values of 5, 10, 20, 30, and 40°C/min.

TABLE II
Nonisothermal Crystallization Parameters of the PP and PPCNs

Sample	φ (°C/min)	n	K_c	$t_{1/2}$ (min)	T_c (°C)	T_P (°C)	ΔH_c (J/g)
PP	5	3.48 ± 0.05	0.47 ± 0.00	1.98	124	118	87.3
	10	3.08 ± 0.11	0.83 ± 0.00	1.37	120	114	86.1
	20	2.99 ± 0.10	1.01 ± 0.00	0.88	116	110	85.0
	30	3.11 ± 0.11	1.04 ± 0.00	0.68	114	108	84.2
	40	3.31 ± 0.08	1.07 ± 0.00	0.56	112	106	84.6
PP/clay 1 1.3 wt %	5	5.09 ± 0.08	0.52 ± 0.00	1.42	125	122	84.0
	10	6.36 ± 0.02	1.06 ± 0.00	1.05	122	118	83.9
	20	4.74 ± 0.05	1.22 ± 0.00	0.70	118	115	85.9
	30	5.12 ± 0.05	1.21 ± 0.00	0.55	116	112	84.7
	40	4.35 ± 0.07	1.17 ± 0.00	0.47	114	110	84.1
PP/clay 2 2.2 wt %	5	3.98 ± 0.14	0.54 ± 0.00	1.31	126	122	80.8
	10	4.98 ± 0.08	0.98 ± 0.01	1.02	122	119	79.8
	20	3.83 ± 0.15	1.09 ± 0.01	0.69	119	115	80.5
	30	3.72 ± 0.17	1.11 ± 0.01	0.54	116	113	80.0
	40	3.68 ± 0.14	1.12 ± 0.01	0.44	115	111	80.5
PP/clay 3 4.8 wt %	5	3.81 ± 0.12	0.60 ± 0.01	1.30	125	121	82.3
	10	3.90 ± 0.12	0.99 ± 0.01	0.97	122	118	85.1
	20	3.75 ± 0.14	1.13 ± 0.01	0.65	118	115	82.9
	30	4.12 ± 0.14	1.15 ± 0.01	0.50	116	113	84.4
	40	3.90 ± 0.10	1.14 ± 0.01	0.42	115	112	85.3

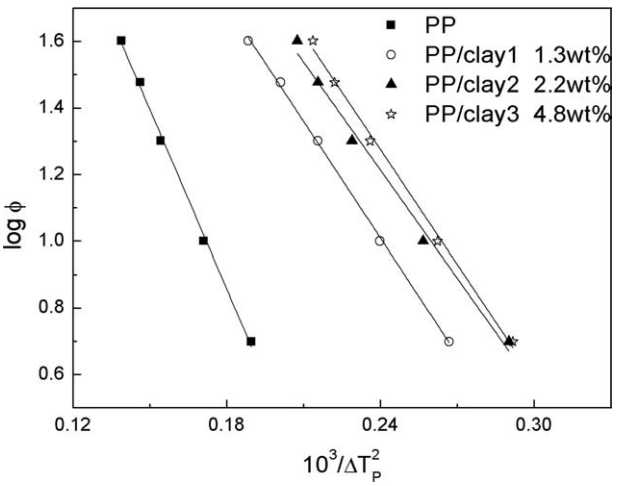

Figure 3 Plots of log ϕ versus $10^3/\Delta T_P^2$ for the PP and PPCNs.

$$\log \phi = A - \frac{B^*}{2.3\Delta T_P^2} \tag{2}$$

where A is a constant; B^* is the B factor in the care of heterogeneous nucleation; ΔT_P is the degree of supercooling, where $\Delta T_P = T_m^0 - T_P$ (where T_m^0 is the equilibrium melting temperature); and B is a factor relating to the three-dimensional nucleation, defined as

$$B = \frac{\omega\sigma^3 V_m^2}{nkT_m\Delta S_m^2} \tag{3}$$

where n is the Kolmogorov–Avrami exponent, ω is a geometrical factor, σ is the specific surface energy, V_m is the molar volume of the crystallizing polymer, ΔS_m is the entropy of melting, and k is Boltzmann's constant.

The nucleation activity (ε) of the filler is defined as the ratio between the three-dimensional work of nucleation with and without filler, $\varepsilon = B^*/B$. If the filler is extremely active for nucleation, ε approaches 0. For absolutely inert particles, ε is 1. Therefore, ε can be directly given by the ratio between the slopes of the linear curves. In this study, the T_m^0 values for commercial PP, PP/clay1, PP/clay2, and PP/clay3 were 191, 183, 181, and 180°C, respectively; this was determined by the Hoffman–Weeks equation.[33] The plots of log ϕ versus $10^3/\Delta T_P^2$ are shown in Figure 3. After linear regression, the slops of PP, PP/clay1,

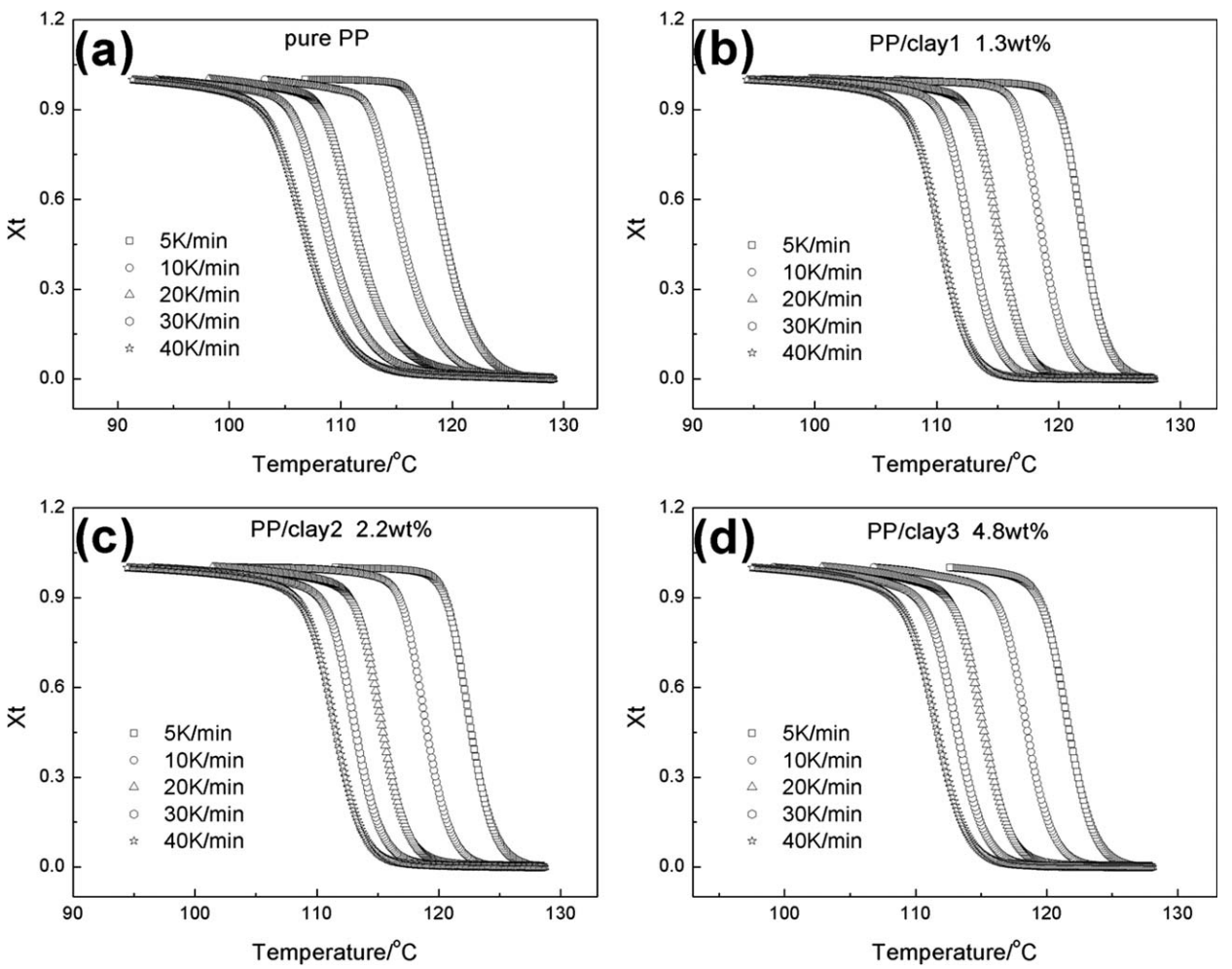

Figure 4 Plots of X_t versus temperature for the PP and PPCNs during the nonisothermal crystallization process.

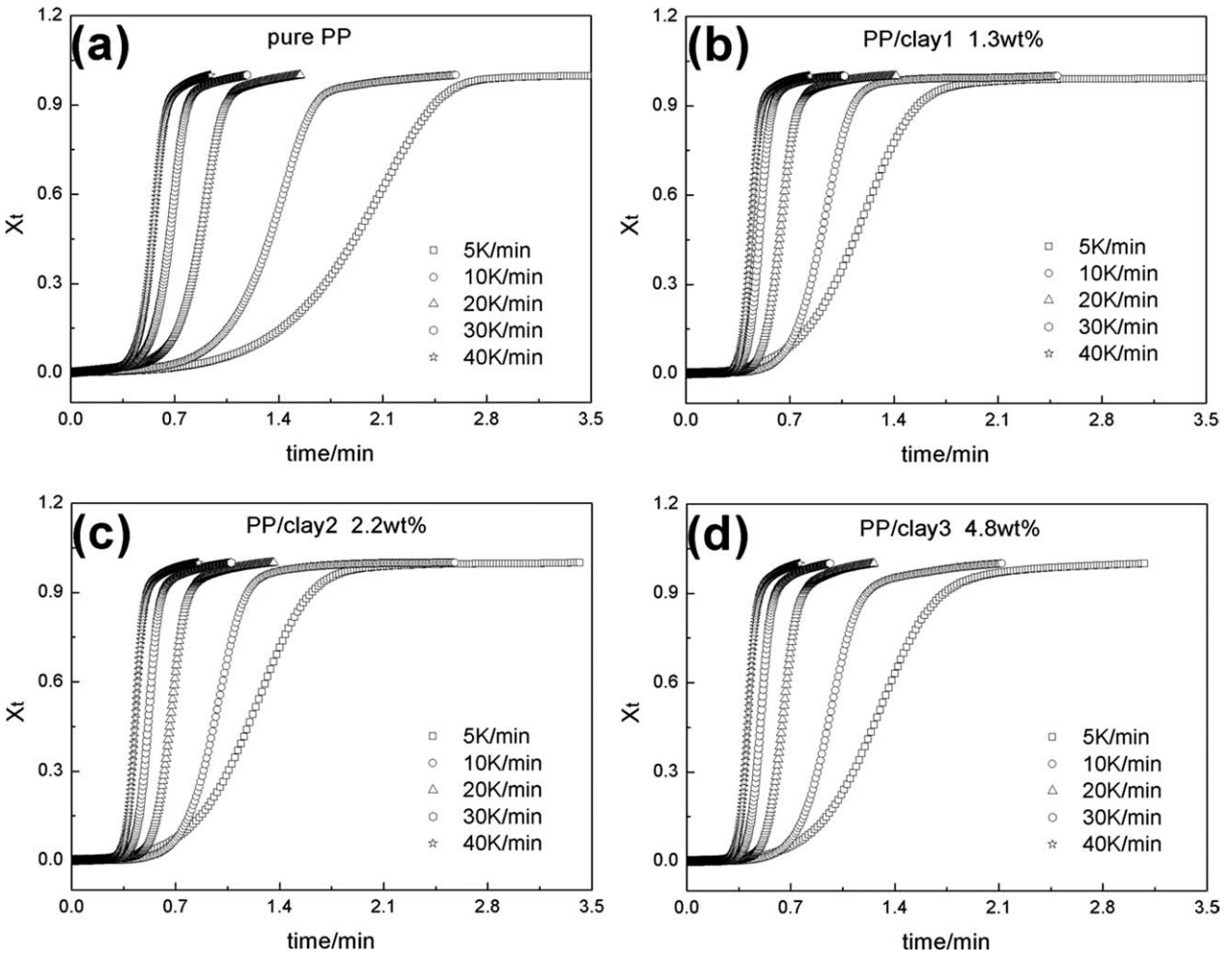

Figure 5 Plots of X_t versus t for the PP and PPCNs during the nonisothermal crystallization process.

PP/clay2, and PP/clay3 were −17.95, −11.68, −10.81, and −11.49, respectively, and the standard errors were 0.490, 0.194, 0.565, and 0.369, respectively. The values of ε for PP/clay1, PP/clay2, and PP/clay3 were 0.65 ± 0.07, 0.60 ± 0.11, and 0.64 ± 0.09, respectively; this demonstrated that in all of the exfoliated PPCN samples, the silicate layers were effective nucleating agents for PP but there was no significant difference between these values. The relationship between ε and the clay structure in the PP matrix is still unclear. The obtained ε values of the PPCNs in this study were a little lower than the 0.71 and 0.84 reported for nylon 1212/MMT[6] and MA–PP/MMT (with a 3 wt % clay content and an intercalated structure), respectively.[36] The T_m^0 of the commercial PP was higher than the T_m^0 of the PP matrix of the PPCNs. This might have resulted in relatively smaller values of ε.

Figure 4 shows the relative crystallinity (X_t) as a function of temperature for the PP and PPCNs at different ϕ values. X_t, as a function of T_c, is defined as follows:

$$X_t = \frac{\int_{T_0}^{T} (dH_c/dT)dT}{\int_{T_0}^{T_\infty} (dH_c/dT)dT} \quad (4)$$

where T_0 and T_∞ are the initial crystallization temperature and the ultimate crystallization temperatures, respectively. The dH_c is the enthalpy of crystalliization released during an infinitesimal temperature range dT.

All of these curves have the same sigmoidal shape, which implies that only the lag effect of ϕ on the crystallization was observed.

Figure 4 can be converted into a time scale with eq. (5):

$$t = \frac{T_0 - T}{\phi} \quad (5)$$

Figure 5 shows that the higher the ϕ value is, the shorter the time is for completing crystallization. The half-time of nonisothermal crystallization ($t_{1/2}$)

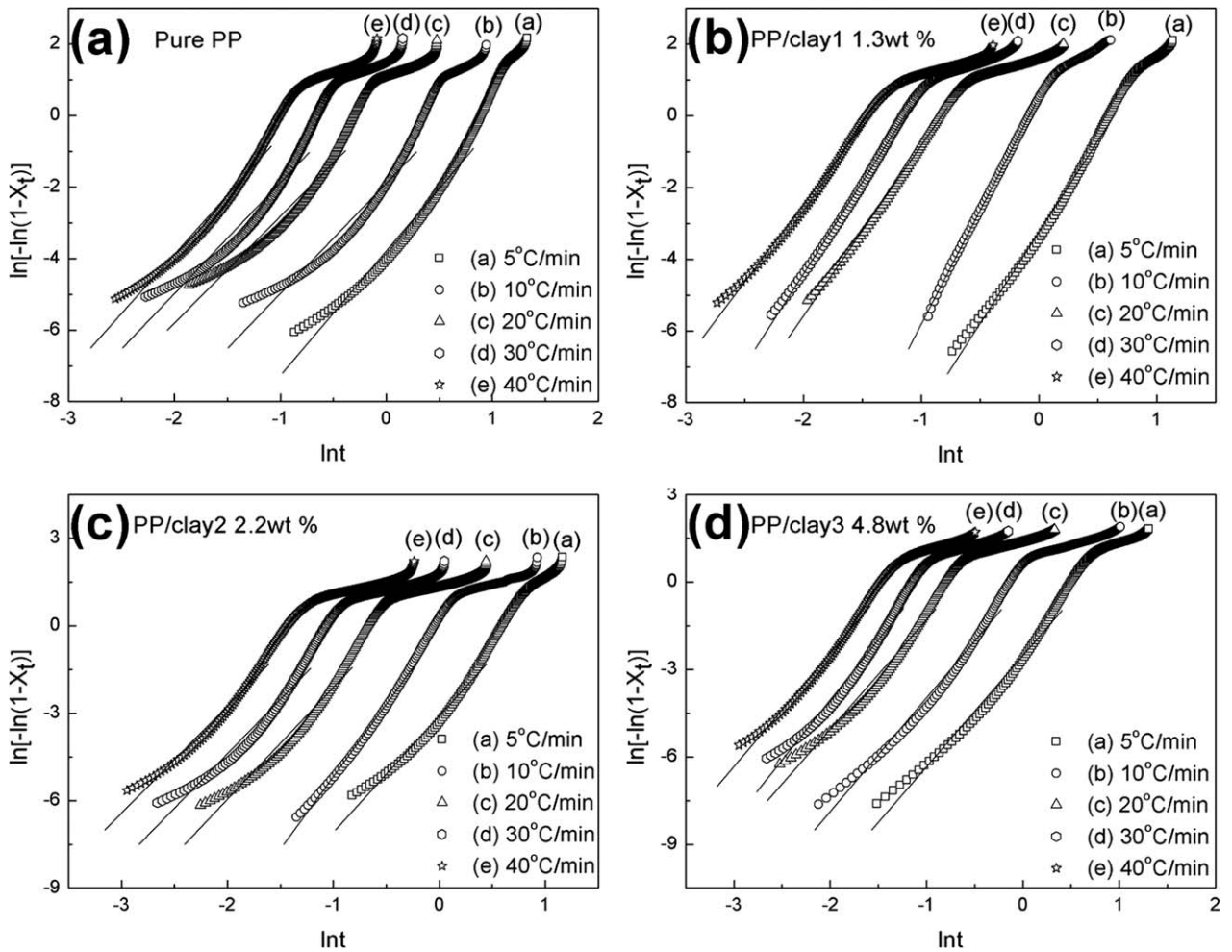

Figure 6 Avrami plots for the PP and PPCNs during the nonisothermal crystallization process.

of the PP and PPCNs was the value of the time when X_t was 50%. This was obtained from Figure 5 and is listed in Table II. As expected, the value of $t_{1/2}$ decreased with increasing ϕ for the PP and PPCNs. Moreover, at a given ϕ, the $t_{1/2}$ values of the PPCNs were smaller than those of PP and decreased as the clay content increased; this indicated that the addition of clay accelerated the overall crystallization process. The higher clay content was, the greater the nucleating effect was, and consequently, the smaller $t_{1/2}$ was.

The Avrami equation [eq. (6)] is commonly used to analyze the isothermal crystallization kinetics of a polymer. It was modified by Jeziorny[29] to describe the nonisothermal kinetics of polymers and polymer composites:[37–45]

$$X_t = 1 - \exp(-K_n T^n) \tag{6}$$

where n is the Avrami exponent, a constant that depends on the type of nucleation and growth process parameters, and K_n is a composite rate constant involving both nucleation and growth rate parameters. If eq. (6) is written in logarithmic form, it appears as follows:

$$\ln[-\ln(1 - X_t)] = \ln K_n + n \ln t \tag{7}$$

When $\ln[-\ln(1 - X_t)]$ versus $\ln t$ was plotted for each φ (Fig. 6) where t is defined by eq. (5), K_n and n in eq. (7) were obtained. In nonisothermal crystallization, K_n and n have different physical meanings from those in isothermal crystallization because of the fact that under nonisothermal crystallization conditions, the temperature changes constantly. This affects the rates of both nuclei formation and spherulite growth because they are temperature dependent. In this case, K_n and n are two adjustable parameters to be fitted to the data. In Table II, the values of n range from 2.99 to 3.48 for PP and from 3.68 to 6.36 for the PPCNs. These results show that the presence of clay changed n. According to the original assumption of the theory,[28] the value of n should be an integer ranging from 1 to 4.

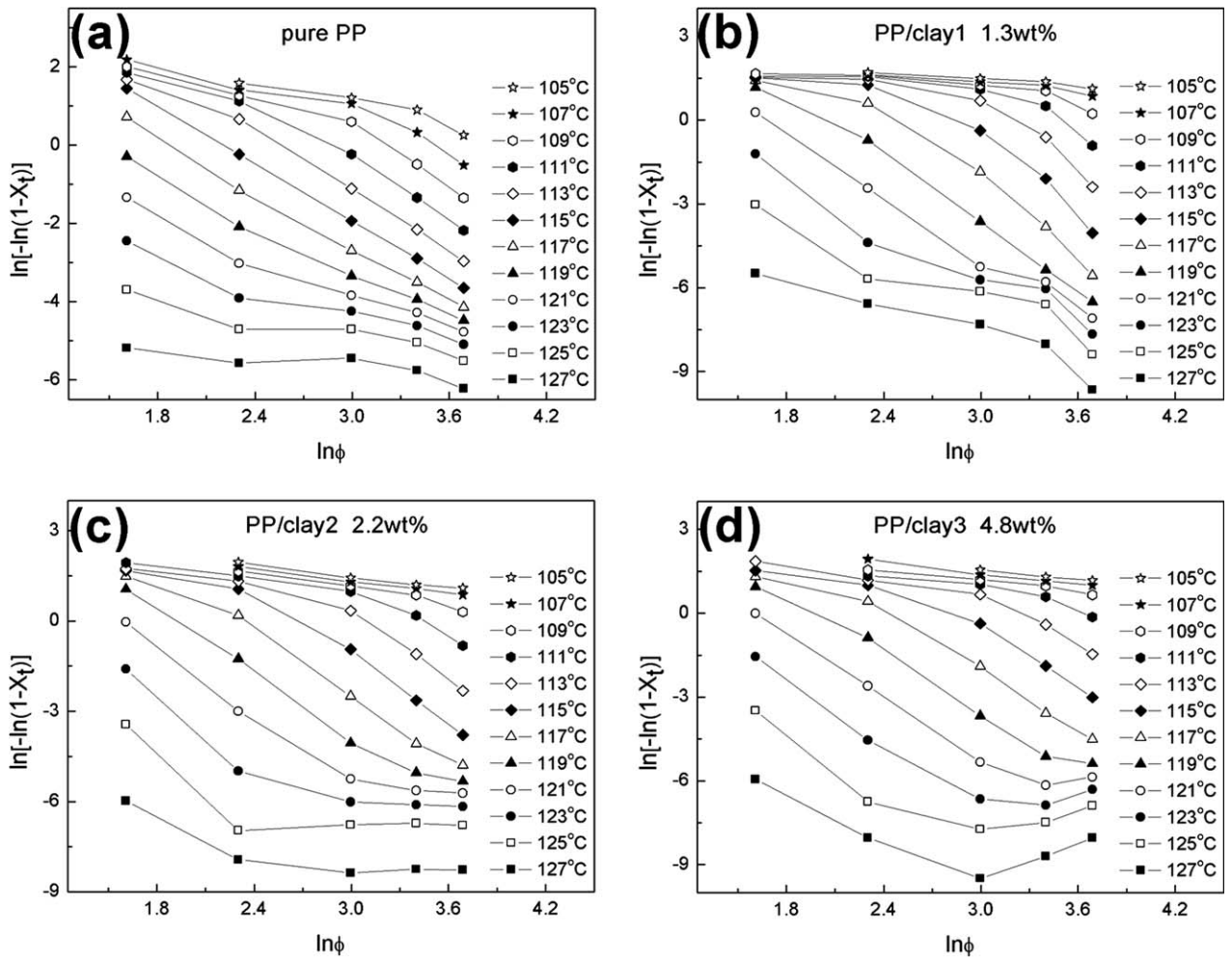

Figure 7 Ozawa plots of $\ln[-\ln(1 - X_t)]$ versus $\ln \phi$ for the crystallization of the PP and PPCNs during the nonisothermal crystallization process.

Nevertheless, nonintegral n values implied that the real crystallization process was more complicated in the PPCNs than the simplification of the Avrami method.

With regard to ϕ, the Jeziorny-modified Avrami equation was used as follows:

$$\ln K_c = \frac{\ln K_n}{\phi} \tag{8}$$

The results obtained from the Avrami plots and Jeziorny method are summarized in Table II. As expected, the value of the crystallization rate constant (K_c) increased with increasing ϕ values for both the PP and PPCNs. At a given temperature, K_c increased as the clay content increased because of the significant nucleating effect of exfoliated silicate layers in the PP matrix.

Assuming that the nonisothermal crystallization process may be composed of infinitesimally small isothermal crystallization steps, Ozawa[30] extended the Avrami equation to the nonisothermal case as follows:

$$1 - X_t = \exp[-K(T)/\phi^m] \tag{9}$$

where $K(T)$ is the Ozawa crystallization rate constant and m is the Ozawa exponent, which depends on the dimensions of crystal growth. Equation (9) in the logarithmic form can be written as follows:

$$\ln[-\ln(1 - X_t)] = \ln K(T) - m \ln \phi \tag{10}$$

By plotting $\ln[-\ln(1 - X_t)]$ versus $\ln \phi$ at a given temperature, one can obtain $K(T)$ and m. The results based on the Ozawa method are illustrated in Figure 7. The nonlinearity of the plots indicated that m was not constant with temperature during the nonisothermal crystallization process. At a given temperature, the curvature of the plot changed. This was because at a given temperature, the crystallization processes at different ϕ values were at different stages, that is, at the lower ϕ, the crystallization process was at the end stage, whereas at the higher ϕ, the crystallization process was at the early stage. In addition, the

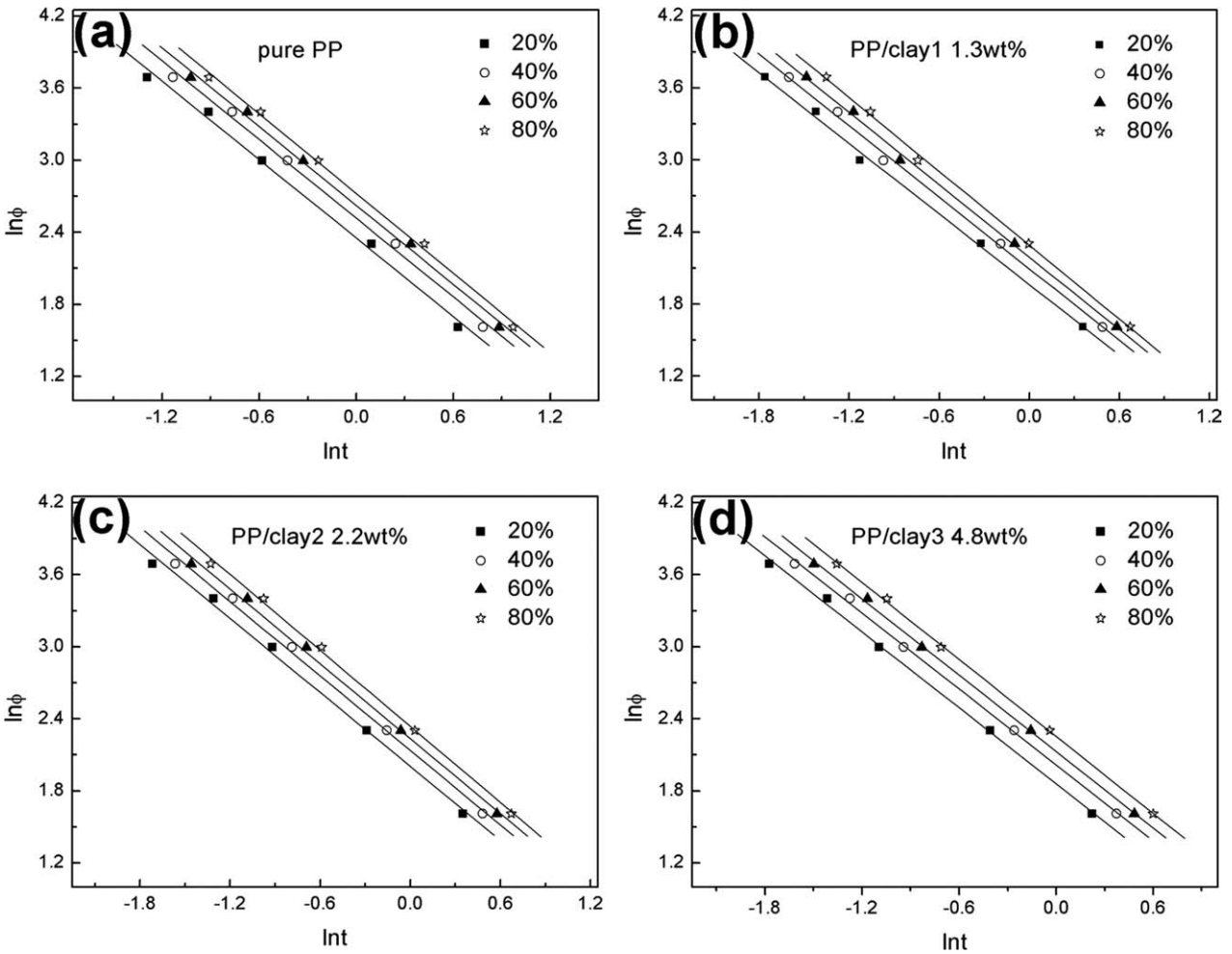

Figure 8 Plots of ln ϕ versus ln t for the PP and PPCNs during the nonisothermal crystallization process.

nonlinearity of the Ozawa model could also be attributed to inaccurate assumptions in theory, such as the occurrence of secondary crystallization, trans-crystallization, and changes in the value of the cooling crystallization function $K(T)$.[46–48] Therefore, the Ozawa equation still could not describe the nonisothermal crystallization process of the PP and PPCNs very well.

A method was proposed by Mo et al.[31] to describe nonisothermal crystallization by the combination of the Avrami equation [eq. (7)] and Ozawa equation [eq. (10)]. In a nonisothermal crystallization process, the Ozawa and Avrami equations are given as follows:

$$\begin{cases} \ln[-\ln(1-X_t)] = \ln K_n + n \ln t \\ \ln[-\ln(1-X_t)] = \ln K(T) - m \ln \phi \end{cases}$$

Their rearrangement at a given X_t produces eq. (11):

TABLE III
Values of $F(T)$ and α for the PP and PPCNs

Sample	X_t (%)	α	$F(T)$	Sample	X_t (%)	α	$F(T)$
PP	20	1.09	10.50	PP/clay2 1.3 wt %	20	1.03	6.57
	40	1.09	12.39		40	1.05	7.50
	60	1.09	13.78		60	1.03	8.61
	80	1.10	15.24		80	1.07	9.51
PP/clay2 2.2 wt %	20	1.03	7.41	PP/clay3 4.8 wt %	20	0.98	7.12
	40	1.03	8.47		40	0.99	8.12
	60	1.04	9.34		60	1.00	8.94
	80	1.06	10.35		80	1.02	9.87

TABLE IV
Kissinger ΔE of the PP and PPCNs

	PP (kJ/mol)	PP/clay1 (kJ/mol)	PP/clay2 (kJ/mol)	PP/clay3 (kJ/mol)
ΔE	219.3 ± 11.5	233.4 ± 29.3	248.0 ± 1.2	267.9 ± 7.1

$$\ln \phi = \ln F(T) - \alpha \ln t \tag{11}$$

where the kinetic parameter $F(T) = [K_n/K(T)]^{1/m}$ refers to the cooling rate φ that needs to be selected within a unit of crystallization time when the measured system reach a certain degree of crystallinity. $\alpha = n/m$ is the ratio of n to m. According to eq. (11), at a given degree of crystallinity, the plot of ln φ versus ln t yields a linear relationship between ln φ and ln t (Fig. 8). The kinetic parameters $F(T)$ and α of PP and PPCNs are listed in Table III.

As shown in Table III, the α values of PP were 1.09–1.10, and the α values of the PPCNs were 0.98–1.07. The values of $F(T)$ increased with increasing X_t for both the PP and PPCNs. At a given X_t, $F(T)$ decreased as the clay content increased. The values of $F(T)$ reflected that in the presence of nanosilicate layers, it was easier for the PP matrix to reach a certain degree of crystallinity within a unit of crystallization time; this indicated that the exfoliated silicate layers, as efficient nucleating agents, facilitated the crystallization kinetics, and this might have been helpful in polymer processing. This method has also been successful for describing the nonisothermal processes of PP and PP/PP-*g*-MAH/MMT,[37] poly(ether ether ketone),[31] poly(β-hydroxybutyrate)-poly(vinyl acetate) blends,[45] and poly(trimethylene terephthalate)/clay nanocomposites.[20]

ΔE of nonisothermal crystallization could be evaluated from the Kissinger method:[32]

$$\frac{d\left[\ln \phi/T_P^2\right]}{d(1/T_P)} = \frac{\Delta E}{R} \tag{12}$$

where R is the universal gas constant. With the plot of ln ϕ/T_P^2 versus $1/T_P$, ΔE was obtained and is listed in Table IV. Figure 9 shows the plots based on the Kissinger method. In previous reports, ΔE of intercalated PPCNs was smaller than that of neat PP,[12,13] although in the exfoliated PPCNs, the values of ΔE exhibited an opposite tendency. It could be explained as follows. The crystallization process of PP contains two parts: the nucleation process and the crystal growth process. The nucleation process is related to the free-energy barrier. The presence of clay reduced the nucleation free-energy barrier and accelerated the crystallization process. This was supported by our former results for $t_{1/2}$ and K_c. The crystal growth process was related to ΔE for the crystalline units transporting across the phase. In the intercalated PPCNs, the nucleation factor might have made a more prominent contribution to ΔE than the latter one because of the relatively large particle size and, therefore, led to the reduction of ΔE after the addition of clay. The crystal growth retardation in PPCNs was related to the content and dispersion degree of clay. In the exfoliated PPCNs, highly exfoliated clay particles, which generated a large amount of nanosilicate layers, hindered the transportation of PP molecules, even at a low clay concentration; therefore, the suppression effect of exfoliated silicate layers on the crystallization process of PP was more significant than that in the intercalated PPCN system. As a result, the value of ΔE in the exfoliated PPCNs increased with the addition of nanoclay particles. A similar phenomenon was also observed in a polyethylene/clay nanocomposite system.[49]

CONCLUSIONS

In this study, we aimed to gain a further understanding of the nonisothermal crystallization behavior of highly dispersed PPCNs. Therefore, exfoliated PPCNs were prepared via an *in situ* polymerization method. ε calculated by Dobreva's method demonstrated that the highly dispersed clay acted as an effective nucleating agent. Kinetic models based on the Avrami, Jeziorny, Ozawa, and Mo methods were used to analyze the nonisothermal crystallization behavior of PP in the exfoliated PPCNs. n, $t_{1/2}$, and

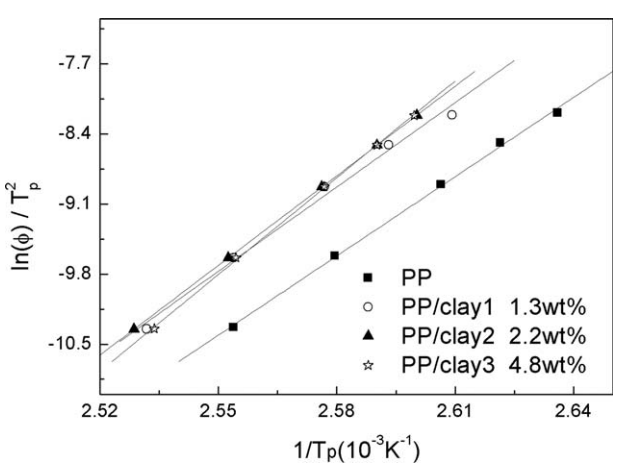

Figure 9 Determination of ΔE for the PP and PPCNs on the basis of the Kissinger method.

K_c were obtained with the former two models. $t_{1/2}$ and K_c satisfactorily described the nucleation effect of clay in the PPCNs, whereas values of n did not provide further information on the nucleation and growth process because the reality was more complicated in the PPCNs than was the simplification of the Avrami method. The Ozawa method failed to provide a constant m; this indicated that m changed during the nonisothermal crystallization process. The Mo method described the nonisothermal crystallization behavior of the PPCNs very well. The ΔE values of the PP and PPCNs determined by the Kissinger method increased with the addition of nanoclay particles. This might have been due to the suppression effect of the highly exfoliated clay on the crystal growth process of PP.

The authors thank Xutao Zhao, Bochao Zhu, Shaoyi Wei, Jijun Jia, and Changjun Zhang from Lanzhou Petrochemical Co. Research Institute (PetroChina) for their cooperation in the propylene autoclave polymerizations.

References

1. Kojima, Y.; Usuki, A.; Kawasumi, M.; Okada, A.; Kurauchi, T.; Kamigaito, O. J Polym Sci Part A: Polym Chem 1993, 31, 983.
2. Lan, T.; Kaviratna, D.; Pinnavaia, T. J. Journal of Physics and Chemistry of Solids, 1996, 57, 1005.
3. Tyan, H. L.; Liu, Y. C.; Wei, K. H. Polymer 1999, 40, 4877.
4. Vaia, R. A.; Jandt, K. D.; Kramer, E. J.; Giannelis, E. P. Chem Mater 1996, 8, 2628.
5. Wu, Z. G.; Zhou, C. X.; Qi, R. R.; Zhang, H. B. J Appl Polym Sci 2002, 83, 2403.
6. Wu, Z. G.; Zhou, C. X.; Zhu, N. Polym Test 2002, 21, 479.
7. Kim, B.; Lee, S. H.; Lee, D.; Ha, B.; Park, J.; Char, K. Ind Eng Chem Res 2004, 43, 6082.
8. Perrin-Sarazin, F.; Ton-That, M. T.; Bureau, M. N.; Denault, J. Polymer 2005, 46, 11624.
9. Ton-That, M. T.; Leelapornpisit, W.; Utracki, L. A.; Perrin-Sarazin, F.; Denault, J.; Cole, K. C.; Bureau, M. N. Polymer Engineering & Science, 2006, 46, 1085.
10. Wang, K.; Liang, S.; Deng, J. N.; Yang, H.; Zhang, Q.; Fu, Q.; Dong, X.; Wang, D. J.; Han, C. C. Polymer 2006, 47, 7131.
11. Wang, K.; Liang, S.; Zhao, P.; Qu, C.; Tan, H.; Du, R. N.; Zhang, Q.; Fu, Q. Acta Mater 2007, 55, 3143.
12. Xu, W. B.; Ge, M. L.; He, P. S. J Polym Sci Part B: Polym Phys 2002, 40, 408.
13. Yuan, Q.; Awate, S.; Misra, R. D. K. Eur Polym J 2006, 42, 1994.
14. Maiti, P.; Nam, P. H.; Okamoto, M.; Hasegawa, N.; Usuki, A. Macromolecules 2002, 35, 2042.
15. Nam, P. H.; Maiti, P.; Okamoto, M.; Kotaka, T.; Hasegawa, N.; Usuki, A. Polymer 2001, 42, 9633.
16. Ma, J. S.; Zhang, S. M.; Qi, Z. N.; Li, G.; Hu, Y. L. J Appl Polym Sci 2002, 83, 1978.
17. Homminga, D.; Goderis, B.; Dolbnya, I.; Reynaers, H.; Groeninckx, G. Polymer 2005, 46, 11359.
18. Kang, X.; He, S. Q.; Zhu, C. S.; Lu, L. W. L.; Guo, J. G. J Appl Polym Sci 2005, 95, 756.
19. Xu, J. T.; Wang, Q.; Fan, Z. Q. Eur Polym J 2005, 41, 3011.
20. Liu, Z. J.; Chen, K. Q.; Yan, D. Y. Eur Polym J 2003, 39, 2359.
21. Homminga, D. S.; Goderis, B.; Mathot, V. B. F.; Groeninckx, G. Polymer 2006, 47, 1630.
22. Fornes, T. D.; Paul, D. R. Polymer 2003, 44, 3945.
23. He, A. H.; Hu, H. Q.; Huang, Y. J.; Dong, J. Y.; Han, C. C. Macromol Rapid Commun 2004, 25, 2008.
24. He, A. H.; Wang, L. M.; Li, J. X.; Dong, J. Y.; Han, C. C. Polymer 2006, 47, 1767.
25. Du, K.; He, A. H. H.; Liu, X.; Han, C. C. Macromol Rapid Commun 2007, 28, 2294.
26. Dobreva, A.; Gutzow, I. J Non-Cryst Solids 1993, 162, 1.
27. Dobreva, A.; Gutzow, I. J Non-Cryst Solids 1993, 162, 13.
28. Avrami, M. J Chem Phys 1940, 8, 212.
29. Jeziorny, A. Polymer 1978, 19, 1142.
30. Ozawa, T. Polymer 1971, 12, 150.
31. Liu, T. X.; Mo, Z. S.; Wang, S. G.; Zhang, H. F. Polym Eng Sci 1997, 37, 568.
32. Kissinger, H. E. J Res Natl Bur Stand 1956, 57, 217.
33. Liu, X.; He, A. H.; Du, K.; Han, C. C. J Polym Sci Part B: Polym Phys 2009, 47, 2215.
34. Fornes, T. D.; Paul, D. R. Polymer 2003, 44, 4993.
35. Van, O. H., Ed. An Introduction to Clay Colloid Chemistry; Wiley (Interscience): New York, 1997.
36. Li, J.; Zhou, C. X.; Gang, W. Polym Test 2003, 22, 217.
37. Xu, W. B.; Liang, G. D.; Zhai, H. B.; Tang, S. P.; Hang, G. P.; Pan, W. P. Eur Polym J 2003, 39, 1467.
38. Liang, G. D.; Xu, J. T.; Xu, W. B. J Appl Polym Sci 2004, 91, 3054.
39. Xu, J. T.; Xue, L.; Fan, Z. Q. J Appl Polym Sci 2004, 93, 1724.
40. Canetti, M.; De Chirico, A.; Audisio, G. J Appl Polym Sci 2004, 91, 1435.
41. Gao, J. G.; Yu, M. S.; Li, Z. T. Eur Polym J 2004, 40, 1533.
42. Weng, W. G.; Chen, G. H.; Wu, D. J. Polymer 2003, 44, 8119.
43. Chen, C.; Fei, B.; Peng, S. W.; Zhuang, Y. G.; Dong, L. S.; Feng, Z. L. Eur Polym J 2002, 38, 1663.
44. Qiu, Z. B.; Mo, Z. S.; Zhang, H. F.; Sheng, S. R.; Song, C. S. J Macromol Sci Phys B 2000, 39, 373.
45. An, Y. X.; Li, L. X.; Dong, L. S.; Mo, Z. S.; Feng, Z. L. J Polym Sci Part B: Polym Phys 1999, 37, 443.
46. Caze, C.; Devaux, E.; Crespy, A.; Cavrot, J. P. Polymer 1997, 38, 497.
47. Di Lorenzo, M. L.; Silvestre, C. Prog Polym Sci 1999, 24, 917.
48. Eder, M.; Wlochowicz, A. Polymer 1983, 24, 1593.
49. Yuan, Q.; Awate, S.; Misra, R. D. K. J Appl Polym Sci 2006, 102, 3809.